

BMP2, BMP4, and BMP7 (9, 10, 26). In dnBMPR-infected limbs, all RNAs are detected at relatively normal levels in the webbed interdigital tissue except *MSX2*, which is at lower levels compared to that in the wild-type limbs (Fig. 5) (20). In all cases, the expression pattern was altered such that these RNAs were detected in soft tissue distal to the truncated digits as well as in the interdigital tissue. In addition, *BMP4* RNA was noticeably absent in mesenchyme surrounding the phalanges of infected limbs at later developmental stages. There is evidence to indicate that *BMP4* regulates its own expression (8, 27). Perhaps the lack of phalangeal expression is related to the reduction in BMP signaling caused by the dnBMPR. *HOXD13*, which may be involved in growth and patterning of the phalanges, was expressed similarly in infected and noninfected limbs at stage 26 and stage 32 of limb development, as was *HOXD11* (Fig. 5) (20, 28).

Here, we used a dominant negative BMP receptor to block BMP signaling in the developing limb. Infection with dnBMPR-IB consistently resulted in a reduction in apoptosis that led to soft tissue syndactyly. Moreover, scales were converted into feathers, and distal development of the digits was affected, leading to loss of the distal phalanges. It was not possible to determine whether the dominant negative BMPR inhibited apoptosis by blocking the action of a single BMP ligand or whether different BMP ligands acted in combination. However, *BMP4* is an attractive candidate for mediating cell death in the limb. Expression of *BMP4* correlates closely with regions of PCD in the limb: the anterior and posterior necrotic zone and the interdigital region. Moreover, *BMP4* has recently been implicated in apoptosis of neural crest cells in the hindbrain in chickens (3). Taken together, this evidence suggests that *BMP4* may play an important role in mediating apoptosis in different tissues at different times during embryogenesis. Moreover, our results indicate that a functional type I BMP receptor is required for BMP-mediated apoptosis. The interdigital region provides a model in vivo system to potentially link an extracellular apoptotic signal and transmembrane receptor kinase to the downstream intracellular cell death machinery.

Note added in proof: Subsequent experiments in our laboratory using chicken dnBMPR-IB (K231R) result in similar phenotypes as infection with the mouse dnBMPR-IB.

REFERENCES AND NOTES

1. S. J. Korsmeyer, *Trends Genet.* **11**, 101 (1995); M. Whyte and G. Evan, *Nature* **376**, 17 (1995).
 2. M. C. Raff, *Nature* **356**, 397 (1992); E. Ruoslahti and J. C. Reed, *Cell* **77**, 477 (1994).
 3. A. Graham, P. Francis-West, P. Brickell, A. Lums-

den, *Nature* **372**, 684 (1994).
 4. J. W. Saunders Jr. and J. F. Fallon, in *Major Problems in Developmental Biology*, M. Locke, Ed. (Academic Press, New York, 1967), pp. 289–314.
 5. V. Garcia-Martinez et al., *J. Cell Sci.* **106**, 201 (1993); Z. F. Zakeri, D. Quagliano, T. Latham, R. A. Lockshin, *FASEB J.* **7**, 470 (1993).
 6. C. E. Milligan et al., *Neuron* **15**, 385 (1995).
 7. K. M. Lyons, R. W. Pelton, B. L. M. Hogan, *Development* **109**, 833 (1990).
 8. C. M. Jones, K. M. Lyons, B. L. M. Hogan, *ibid.* **111**, 531 (1991).
 9. P. H. Francis, M. K. Richardson, P. M. Brickell, C. Tickle, *ibid.* **120**, 209 (1994).
 10. P. H. Francis-West et al., *Dev. Dyn.* **203**, 187 (1995).
 11. K. M. Lyons, B. L. M. Hogan, E. J. Robertson, *Mech. Dev.* **50**, 71 (1995).
 12. F. Liu, F. Ventura, J. Doody, J. Massagué, *Mol. Cell Biol.* **15**, 3479 (1995).
 13. B. L. Rosenzweig et al., *Proc. Natl. Acad. Sci. U.S.A.* **92**, 7632 (1995).
 14. J. L. Wrana, L. Attisano, R. Wieser, F. Ventura, J. Massagué, *Nature* **370**, 341 (1994).
 15. B. B. Koenig et al., *Mol. Cell Biol.* **14**, 5961 (1994); P. ten Dijke et al., *J. Biol. Chem.* **269**, 16985 (1994).
 16. H. Zou, L. Niswander, F. Ventura, J. Massagué, unpublished observations.
 17. J. Carcamo et al., *Mol. Cell Biol.* **14**, 3810 (1994).
 18. S. H. Hughes, J. J. Greenhouse, C. J. Petropoulos, P. Sutcliffe, *J. Virol.* **61**, 3004 (1987).
 19. The gene encoding mouse BMPR-IB was subjected to site-directed oligo mutagenesis (Clontech) to change Lys²³¹ to Arg. This was cloned into a Cla12Nco shuttle vector and then into the replication-competent avian retroviral vector RCAS(A) (18). Primary chick embryo fibroblasts were transfected with the use of lipofectin (Gibco-BRL), culture supernatant was collected on days 6 to 10, and the virus was concentrated by centrifugation, resuspended in a small volume, aliquoted, and stored at -70°C. The concentration of virus was estimated on the basis of reverse transcriptase assays (>1 × 10⁹ units of reverse transcriptase per microliter of concentrated stock), which correlates to ~1 × 10¹¹ plaque-forming units per milliliter of concentrated stock as titered

on our indicator virus. Four virus preparations were used for these studies with similar results.
 20. H. Zou and L. Niswander, unpublished observations.
 21. M.-P. Pautou, *J. Embryol. Exp. Morphol.* **34**, 511 (1975).
 22. D. Dhouailly, M. H. Hardy, P. Sengel, *ibid.* **58**, 63 (1980).
 23. D. M. Kingsley et al., *Cell* **71**, 399 (1992); E. E. Stom et al., *Nature* **368**, 639 (1994).
 24. G. Winnier, M. Blessing, P. A. Labosky, B. L. M. Hogan, *Genes Dev.* **9**, 2105 (1995).
 25. Y. Ishidou et al., *J. Bone Miner. Res.* **10**, 1651 (1995).
 26. B. Robert, G. Lyons, B. K. Simandl, A. Kuroiwa, M. Buckingham, *Genes Dev.* **5**, 2363 (1991); M. A. Ros, D. Macias, J. F. Fallon, J. M. Hurler, *Anat. Embryol.* **190**, 375 (1994).
 27. S. Vainio, I. Karavanova, A. Jowett, I. Thesleff, *Cell* **75**, 45 (1993).
 28. J.-C. Izpisua-Belmonte, C. Tickle, P. Dollé, L. Wolpert, D. Duboule, *Nature* **350**, 585 (1991).
 29. V. Hamburger and H. Hamilton, *J. Morphol.* **88**, 49 (1951).
 30. D. G. Wilkinson, in *In Situ Hybridization*, D. G. Wilkinson, Ed. (Oxford Univ. Press, Oxford, 1993), pp. 75–83.
 31. B. Houston, B. H. Thorp, D. W. Burt, *J. Mol. Endocrinol.* **13**, 289 (1994).
 32. We are grateful to K. Miyazono for the gene encoding mouse BMPR-IB, J. Massagué and F. Ventura for receptor construct design and for performing the in vitro kinase assay, and K. Manova of the Memorial Sloan-Kettering Cancer Center Molecular Cytology Facility. Probes were kindly provided by B. Robert (*MSX1* and *MSX2*), P. Brickell (*BMP2* and *BMP4*), B. Houston (*BMP7*), and J.-C. Izpisua-Belmonte (*HOXD13*). We thank our lab members, B. Hogan and J. Massagué, for critical reading of the manuscript and S. Noramly for advice on the scale-to-feather transformation. This work was supported by Memorial Sloan-Kettering Cancer Center Support Grant and American Cancer Society Junior Faculty Research Award.

2 January 1996; accepted 29 March 1996

Role of Gene Interactions in Hybrid Speciation: Evidence from Ancient and Experimental Hybrids

Loren H. Rieseberg,* Barry Sinervo, C. Randal Linder, Mark C. Ungerer, Dulce M. Arias

The origin of a new diploid species by means of hybridization requires the successful merger of differentiated parental species' genomes. To study this process, the genomic composition of three experimentally synthesized hybrid lineages was compared with that of an ancient hybrid species. The genomic composition of the synthesized and ancient hybrids was concordant ($r_s = 0.68$, $P < 0.0001$), indicating that selection to a large extent governs hybrid species formation. Further, nonrandom rates of introgression and significant associations among unlinked markers in each of the three synthesized hybrid lineages imply that interactions between coadapted parental species' genes constrain the genomic composition of hybrid species.

Reduced hybrid fertility or viability appears to result from unfavorable interactions between parental species' genomes

L. H. Rieseberg, B. Sinervo, C. R. Linder, M. C. Ungerer, Department of Biology, Indiana University, Bloomington, IN 47405, USA.
 D. M. Arias, Centro de Investigación Ambiental E Investigación Sierra de Huautla, Universidad Autónoma del Estado de Morelos, Cuernavaca, Morelos, Mexico 62210.

*To whom correspondence should be addressed.

(1). As a result, species' genomes are considered to be coadapted and thereby resistant to the introgression of alien genes (1). However, the successful origin of new diploid species by means of hybridization raises the possibility that interactions between parental species' genes are not universally unfavorable (2). Little is known about the strength and fitness consequences of gene interactions in hybrids or their role in hybrid speciation (3). Here we compare

the genomic composition of three experimentally synthesized hybrid lineages (*Helianthus annuus* × *H. petiolaris*) with that of an ancient hybrid species (*H. anomalus*) (4) to determine whether the genetic factors governing the genomic composition of artificial hybrids are similar to those involved in hybrid speciation. We then analyze parental marker segregation in the experimentally synthesized hybrid lineages to detect interactions among genes that affect hybrid fitness and, indirectly, hybrid genomic composition.

The three sunflower species studied here are self-incompatible annuals native to North America (5). The parents, *H.*

annuus and *H. petiolaris*, are common in the western United States (5). Although differing in karyotype, morphology, and habitat requirements, they frequently grow together, and hybrid swarms are common (6). First generation hybrids are semisterile, but full fertility can be regained in later generation hybrids (6). The stabilized hybrid, *H. anomalus*, is restricted to xeric habitats in northern Arizona and southern Utah, well within the range of its parental species (7). Although morphologically distinct (7), it combines parental ribosomal DNA-repeat units, allozymes, chloroplast DNA haplotypes, and random amplified polymorphic DNA (RAPD)

markers (4, 8). The near absence of ribosomal DNA and chloroplast DNA sequence divergence between *H. anomalus* and its parents suggests a recent origin of the hybrid species, probably within the last 170,000 years (8). Reproductive isolation between *H. anomalus* and its parental species has been facilitated by rapid karyotypic evolution (4).

To study the genetic processes accompanying hybrid speciation, we synthesized three hybrid lineages between *H. annuus* and *H. petiolaris*: lineage I, P-F₁-BC₁-BC₂-F₂-F₃; lineage II, P-F₁-F₂-BC₁-BC₂-F₃; and lineage III, P-F₁-F₂-F₃-BC₁-BC₂ (9). For each hybrid lineage, total DNA was isolated from 56 or 58 progeny from the final generation (10), and these 170 DNAs were surveyed for 197 *H. petiolaris* RAPD markers of known genomic location (4, 10). On completion of the marker survey, *H. petiolaris* markers present in the hybrid lineage were plotted onto the genomic map of *H. annuus*, thereby generating a graphical genotype (11) for each hybrid lineage (Fig. 1).

Concordance in genomic composition among the three synthesized hybrid lineages was tested by comparing distributions of introgressed *H. petiolaris* markers (Fig. 1). Patterns of introgression were strongly correlated among the three synthesized lineages [(12); ($P < 0.0001$ for all combinations)], indicating that to a large extent selection rather than chance governs the genomic composition of hybrids between *H. annuus* and *H. petiolaris*.

To determine whether the genomic composition of the synthesized hybrids was concordant with that of the ancient hybrid species, *H. anomalus*, we compared the distribution of species-specific markers in the *H. anomalus* genome (4) to the distribution of parental genomic regions in the synthesized hybrids (Fig. 2). The genomic composition of the ancient hybrid species was recognizably similar to that of experimental hybrid lineages [(13); ($r_s = 0.68$, $N = 140$, $P < 0.0001$)], suggesting that genomic structure and composition of hybrid species may be essentially fixed within a few generations after the initial hybridization event and remain relatively static thereafter (14).

Several genetic factors appear to govern hybrid genomic composition. First, the parental species are chromosomally divergent, and certain rearranged linkage blocks (for example, linkage group T) appear to resist recombination in both the experimental and ancient hybrids (Figs. 1 and 2). Moreover, because all backcrosses in the synthesized hybrids were in the direction of *H. annuus*, chromosomal rearrangements to a large extent account for the low frequency of *H. petiolaris* markers

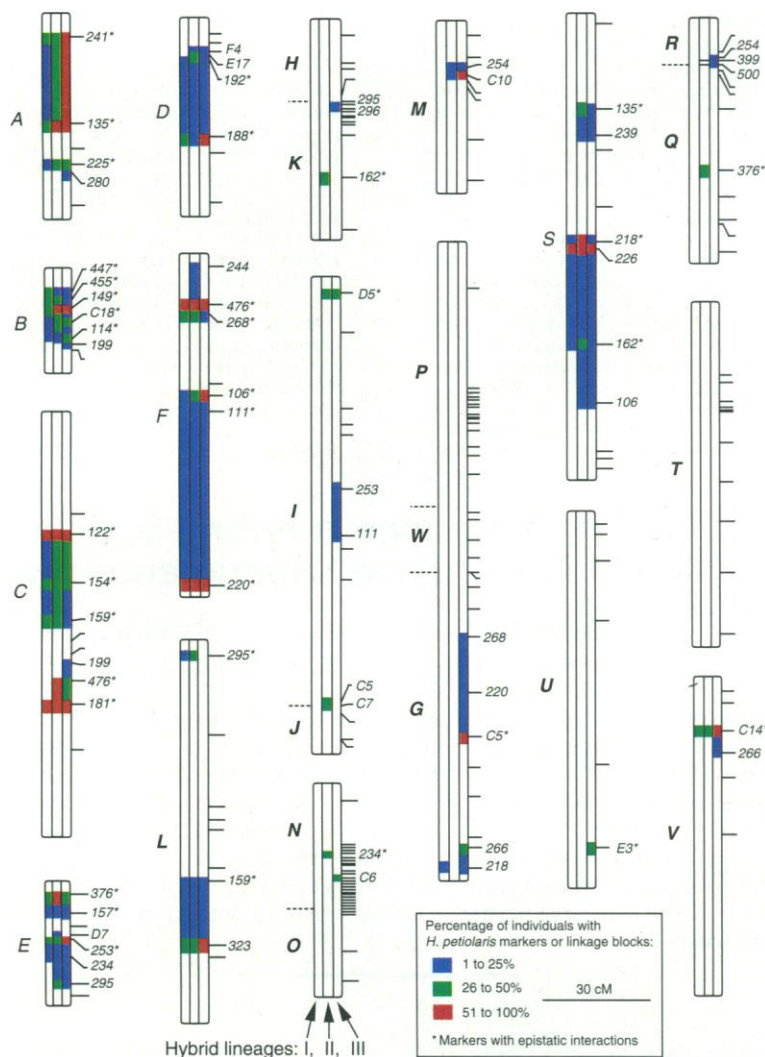


Fig. 1. Composite graphical genotypes of three experimentally synthesized hybrid lineages. Graphical genotypes for hybrid lineages I, II, and III are in the left, center, and right side, respectively, of each linkage group. The graphical genotypes are based on the 1084-cM map of *H. annuus*, extended here by ~290 cM because several *H. petiolaris* markers occur outside currently mapped regions in *H. annuus* (4). Letters at the left of each linkage group designate major linkage blocks and indicate their relation to homologous linkages in *H. petiolaris* (4). These letters also indicate whether the linkage groups are collinear (normal type) or rearranged (bold type) between the parental species (4). Horizontal lines extending to the right of linkage groups indicate the genomic location of the 197 *H. petiolaris* RAPD markers surveyed (10); introgressed markers are identified by primer number. Because of dominance, we often were unable to determine whether the *H. petiolaris* markers or segments were present in the homozygous or heterozygous condition.

fitness of hybrids between *H. annuus* and *H. petiolaris* appears to result from reduced fertility; F_1 's exhibit pollen viabilities of less than 10% and seed set less than 1% (6). In this experiment, uniformly high

fertility (>90% pollen viability) was recovered by the fifth generation in all three synthesized hybrid lineages. Thus, many of the gene interactions reported may affect hybrid fertility. Interspecific competition

among viable pollen grains also serves as a reproductive barrier between *H. annuus* and *H. petiolaris* (20), so some of the epistatic gene combinations observed here possibly affect pollen tube growth rates. Further study will focus on identifying fitness traits physically linked to these markers.

Interactions between divergent species' genomes are often viewed as uniformly disharmonious (1), resulting in hybrid inviability or sterility. The data presented here suggest that although the majority of interspecific gene interactions are indeed unfavorable or neutral, a small percentage of alien genes do appear to interact favorably in hybrids. These favorable gene interactions might provide the raw material for adaptive evolution in hybrid taxa. Although we detected gene interactions in interspecific crosses, it seems plausible that with much larger progenies, this approach might also be useful for estimating genome-wide fitness epistasis within species or populations.

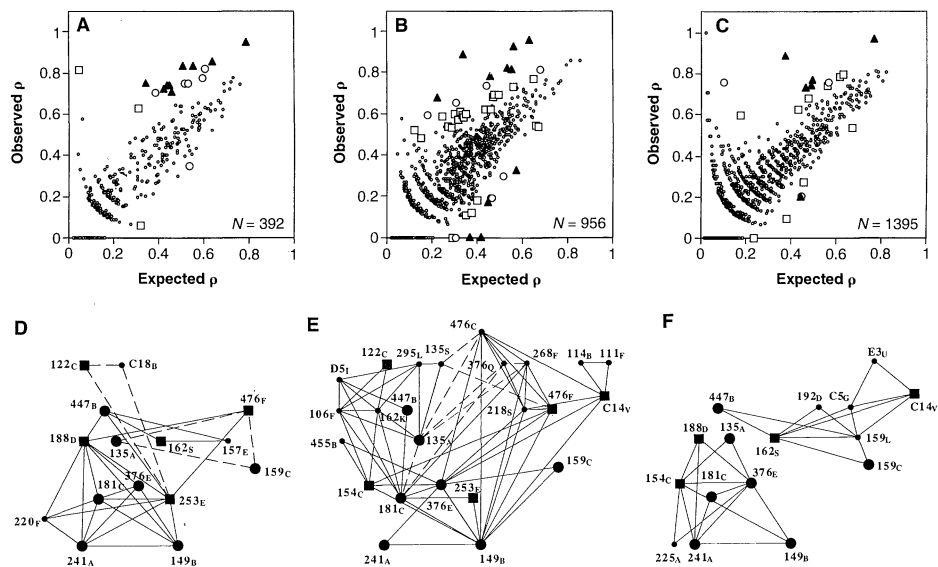


Fig. 3. Epistatic interactions among introgressed *H. petiolaris* markers in synthesized hybrid lineages. (A through C) Scatter plots of observed and expected ρ 's, a measure of association (18), for two-way epistatic interactions in hybrid lineages I (A), II (B), and III (C). N is the total number of two-way associations. (\blacktriangle) $P < 0.0001$; (\circ) $P \leq 0.001$; (\square) $P \leq 0.01$; (\circ) not significant. Symbols (\blacktriangle , \circ , \square) above the cluster of nonsignificant interactions (\circ) are positive associations (21); symbols below are negative associations (22). (D through F) "Webs" of significant three-way epistatic interactions ($P \leq 0.0001$) for hybrid lineages I (D), II (E), and III (F) as indicated by triangles connecting three unlinked markers. Marker designations indicate primer number and linkage block (compare with Fig. 1). Any three markers that interacted epistatically are connected as a triangle. (\bullet) Markers involved in three-way epistatic interactions in all three hybrid lineages; (\blacksquare) markers involved in three-way epistatic interactions in two hybrid lineages; (\bullet) markers involved in three-way epistatic interactions in one hybrid lineage. Lengths connecting markers are arbitrary. Positive associations are indicated by solid lines and negative associations by dashed lines. For example, the three unlinked markers 241_A, 149_B (both at the base of all three webs) (D through F), and marker 376_E (web interior) were positively associated in all three hybrid lineages, as indicated by the connecting triangle.

Table 1. Observed and expected proportions of markers introgressed into 0%, 1 to 25%, 26 to 50%, and >50% of individuals.

| Percentage of individuals in which markers introgressed | Entire genome (197 markers) | | Collinear portion (58 markers) | | Rearranged portion (139 markers) | |
|---|-----------------------------|-----------|--------------------------------|----------|----------------------------------|----------|
| | Observed | Expected* | Observed | Expected | Observed | Expected |
| <i>Hybrid lineage I</i> | | | | | | |
| 0 | 0.85 | 0.0009 | 0.57 | 0.0006 | 0.96 | 0.0008 |
| 1 to 25 | 0.07 | 0.9662 | 0.17 | 0.9755 | 0.02 | 0.9656 |
| 26 to 50 | 0.06 | 0.0329 | 0.17 | 0.0239 | 0.01 | 0.0336 |
| >50 | 0.03 | <0.0001 | 0.09 | <0.0001 | 0.0 | <0.0001 |
| <i>Hybrid lineage II</i> | | | | | | |
| 0 | 0.76 | 0.0001 | 0.40 | 0.0003 | 0.91 | 0.0003 |
| 1 to 25 | 0.08 | 0.8868 | 0.19 | 0.8596 | 0.03 | 0.8746 |
| 26 to 50 | 0.12 | 0.1131 | 0.24 | 0.1401 | 0.06 | 0.1251 |
| >50 | 0.05 | <0.0001 | 0.17 | <0.0001 | 0.0 | <0.0001 |
| <i>Hybrid lineage III</i> | | | | | | |
| 0 | 0.71 | <0.0001 | 0.38 | <0.0001 | 0.85 | <0.0001 |
| 1 to 25 | 0.17 | 0.5080 | 0.32 | 0.4443 | 0.11 | 0.4880 |
| 26 to 50 | 0.05 | 0.4920 | 0.12 | 0.5557 | 0.02 | 0.5120 |
| >50 | 0.07 | <0.0001 | 0.17 | <0.0001 | 0.02 | <0.0001 |

*Expected values were calculated with the mean SD calculated from the SDs of 100 simulations of unrestricted marker introgression for the entire genome, as well as within the collinear and rearranged portions of the genome (10). Hybrid lineage I: 0.156 \pm 0.0504 (mean \pm SD); hybrid lineage II: 0.1878 \pm 0.0515; hybrid lineage III: 0.2487 \pm 0.0578.

REFERENCES AND NOTES

1. E. Mayr, *Animal Species and Evolution* (Belknap, Cambridge, 1963); H. L. Carson, *Am. Nat.* **109**, 83 (1975); A. R. Templeton, *Genetics* **94**, 1011 (1980).
2. M. L. Arnold and S. A. Hodges, *Tree* **10**, 67 (1995); L. H. Rieseberg, *Am. J. Bot.* **82**, 944 (1995).
3. R. G. Harrison, *Oxford Surv. Evol. Biol.* **7**, 69 (1990).
4. L. H. Rieseberg, C. Van Fossen, A. M. Desrochers, *Nature* **375**, 313 (1995).
5. C. B. Heiser, D. M. Smith, S. Clevenger, W. C. Martin, *Mem. Torrey Bot. Club* **22**, 1 (1969).
6. C. B. Heiser, *Evolution* **1**, 249 (1947).
7. ———, *Rhodora* **60**, 271 (1958); G. P. Nabhan and K. L. Reichhardt, *Southwest. Nat.* **28**, 231 (1983).
8. L. H. Rieseberg, *Am. J. Bot.* **78**, 1218 (1991); ———, S. Beckstrom, A. Liston, D. Arias, *Syst. Bot.* **16**, 50 (1991); L. H. Rieseberg, H.-C. Choi, R. Chan, C. Spore, *Heredity* **70**, 285 (1993).
9. The initial interspecific cross was *H. annuus* (cmsHA89; female) \times *H. petiolaris* subsp. *petiolaris* (PET-PET-1741; male). Backcrosses were in the direction of *H. annuus*, the maternal parent, because more of the *H. anomalus* genome is derived from *H. annuus* than from *H. petiolaris*. As a result of self-incompatibility, sib-mating rather than selfing was used for the F generations. At least 20 plants were used for each generation. Crosses were performed by applying pooled pollen from all plants from a given generation to stigmas of the same individuals. All achenes produced from each generation were pooled, and 30 achenes were arbitrarily chosen as founders of the next generation. With the exception of the parents and F_1 's, each hybrid lineage was generated independently.
10. L. H. Rieseberg, C. R. Linder, G. Seiler, *Genetics* **141**, 1163 (1995).
11. N. D. Young and S. D. Tanksley, *Theor. Appl. Genet.* **77**, 95 (1989).
12. Spearman's rank correlation coefficient was calculated for each pairwise combination of the three hybrid lineages. Patterns of introgressed and nonintrogressed markers were compared, such that *H. petiolaris* markers present in at least one of the progeny from a given lineage were scored as introgressed. Lineages I \times II, $r_s = 0.88$, $P < 0.0001$; lineages I \times III, $r_s = 0.82$, $P < 0.0001$; lineages II \times III, $r_s = 0.83$, $P < 0.0001$.
13. Concordance between the genomic composition of the experimental and ancient hybrids was calculated with the use of Spearman's rank correlation coefficient for the entire, collinear, and rearranged portions of the genome. For the experimental hybrids, linkage blocks introgressed in one or more individuals in any

Origin of Replication of *Mycoplasma genitalium*

- of the synthesized hybrids were considered *H. petiolaris* genomic regions (1), whereas linkage blocks lacking *H. petiolaris* markers were designated *H. annuus* regions (0), thereby generating the composite distribution of parental genomic regions shown in Fig. 2. Parental markers in *H. anomalus* either matched (0,0 or 1,1) or did not match (0,1 or 1,0) the corresponding genomic region in the experimental hybrids.
14. E. M. McCarthy, M. A. Amussen, W. W. Anderson, *Heredity* **74**, 502 (1995); V. Grant, *Genetics* **54**, 1189 (1966).
 15. Spearman's rank correlation coefficient was calculated for each pairwise combination of the three hybrid lineages. The percentage at which a marker introgressed for a given lineage was scored in the following manner: 0.0% = 0; 1 to 25% = 1; 26 to 50% = 2; 51 to 100% = 3. Lineages I × II, $r_s = 0.79$, $P < 0.0001$; lineages I × III, $r_s = 0.74$, $P < 0.0001$; lineages II × III, $r_s = 0.73$, $P < 0.0001$.
 16. N. H. Barton and G. M. Hewitt, *Heredity* **47**, 367 (1981).
 17. C.-I. Wu and M. F. Palopoli, *Annu. Rev. Genet.* **27**, 283 (1994).
 18. The following equation was used to compute the test statistic (ρ) for two-way epistatic interactions among unlinked loci (N_{loci} , number of unlinked loci; $N_{progeny}$, number of progeny tested; and $locus_{n,p} = 0$ if the *H. petiolaris* marker is absent and 1 if present):

$$\rho_{i \times j} = \frac{\sum_{p=1}^{N_{progeny}} \prod_{n=1}^{N_{loci}} locus_{n,p}}{\sqrt{\sum_{p=1}^{N_{progeny}} locus_{i,p} \times \sum_{p=1}^{N_{progeny}} locus_{j,p}}}$$

where $0 \leq \rho_{i \times j} \leq 1$ (1)

Equation (1) can be generalized to *N*-way epistatic interactions:

$$\rho_{1 \times \dots \times N_{loci}} = \frac{\sum_{p=1}^{N_{progeny}} \prod_{n=1}^{N_{loci}} locus_{n,p}}{N_{loci} \sqrt{\prod_{n=1}^{N_{loci}} \sum_{p=1}^{N_{progeny}} locus_{n,p}}}$$

where $0 \leq \rho_{i \times j} \leq 1$ (2)

Significance for each two- or three-way association was tested by comparing $\rho_{observed}$ with $\rho_{expected}$ as computed by bootstrap randomization of the observed data ($N = 10,000$ per association) (Fig. 3).

19. Seventy-four percent of epistatic markers were found in all three lineages in contrast to 10% of nonepistatic markers ($G^2 = 30.6$, $df = 2$, $P < 0.0001$). However, part of this correlation may be due to the greater power of the ρ test statistic in detecting associations among markers of intermediate frequency.
20. L. H. Rieseberg, A. M. Desrochers, S. J. Youn, *Am. J. Bot.* **82**, 515 (1995).
21. Positive two-way associations occur when unlinked *H. petiolaris* markers appear together within individuals of the progeny array more often than would be expected by chance, suggesting nonadditive, positive fitness effects (for example, increased pollen viability) when these markers appear together. By contrast, negative associations occur when unlinked *H. petiolaris* markers appear together less often than would be expected by chance, suggesting nonadditive negative fitness effects when these markers appear together.
22. Positive three-way associations are similar to two-way associations (21), except that three *H. petiolaris* markers are involved. Negative three-way associations may consist of negative two-way associations only or a combination of negative and positive two-way associations.
23. We thank M. Debacon, G. Valladares, and D. Salinas for technical assistance and J. Whitton, C. Lively, and N. Barton for helpful comments on an earlier version of the manuscript. Supported by National Science Foundation (NSF) grant BSR-9419206 and USDA 92373007590 (to L.H.R.) and NSF BIR-9411128 (to C.R.L.).

18 December 1995; accepted 29 February 1996

The complete sequence of the genome of *Mycoplasma genitalium* was reported and analyzed by Claire M. Fraser *et al.* (1). The origin of replication of the chromosome was not localized precisely because of the lack of consensus patterns, "DnaA boxes," in this species, but it was suggested that the origin might be in an untranscribed AT-rich region between *dnaA* and *dnaN*. This location can be confirmed using a new method based on the results of the mathematical analysis of the model of DNA evolution under no-strand-bias conditions (2)—that is, when there is no strand-bias for the mutation process or for the selective process between the two strands of DNA.

Under no-strand-bias conditions, the

equilibrium point is such that the base frequencies in each strand always respect $[A]=[T]$ and $[C]=[G]$ equalities, regardless of the initial state of the DNA sequence and of details of the substitution patterns. Any significant deviation from the intra-strand rules $[A]=[T]$ or $[C]=[G]$ is an indication that there is an inequality in the substitution patterns between the two strands of DNA. The null hypothesis for the detection of such an inequality is then the appearance of intra-strand equilibrium frequencies $[A]=[T]$ and $[C]=[G]$. Because the mechanisms for DNA replication differ between the leading strand and the lagging strand (3), at least in vitro, mutation patterns could differ depending on

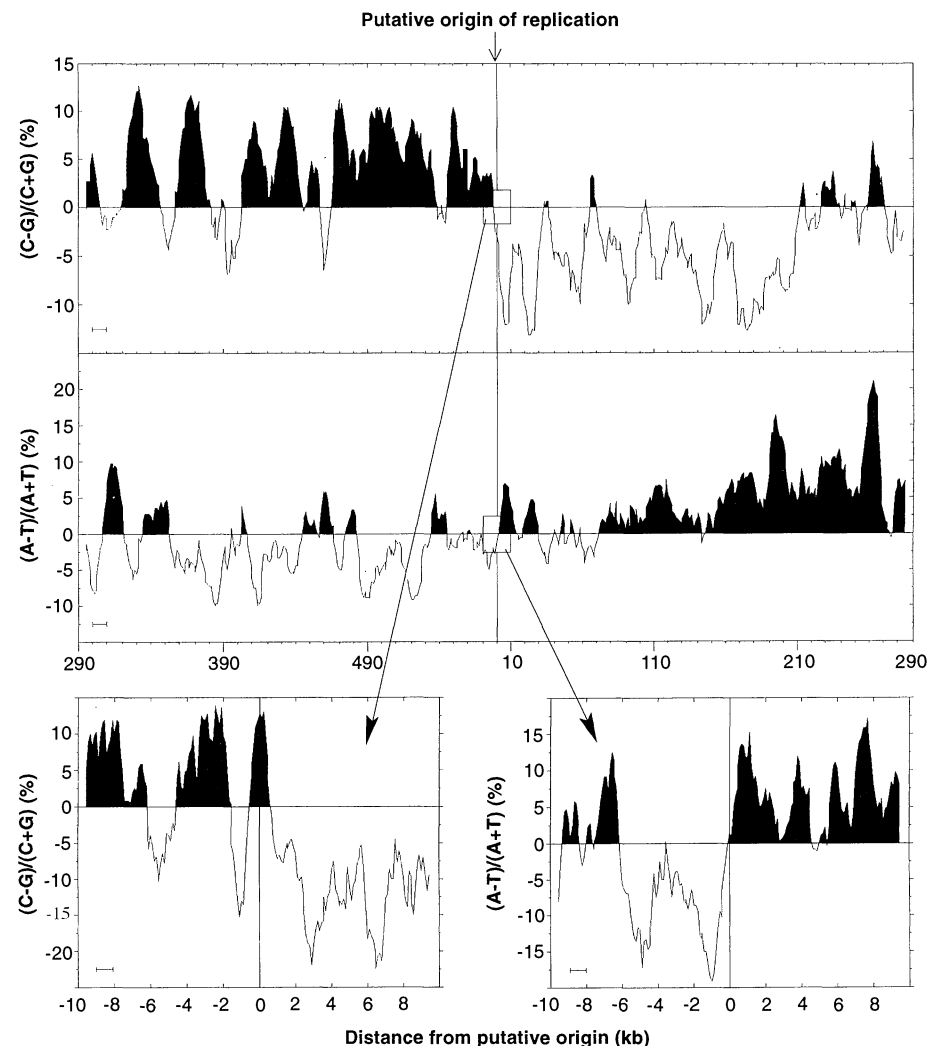


Fig. 1. Origin of replication in *M. genitalium*, showing switch of polarity of base composition asymmetries. Moving window size and step: top 10 kb, 1 kb; bottom 1 kb, 0.1 kb. Each data point is at the middle of its window.